



BEHAVIOR OF COMPOSITE REINFORCED CONCRETE STEEL COLUMNS CONFINED WITH DIFFERENT SHAPES OF STIRRUPS AND STEEL WIRE MESH

Ezz-Eldeen, H. A.

Associate Prof., Civil Eng. Dept, Faculty of Engineering, Al-Azhar university, Cairo, Egypt.

الملخص العربي :

يهدف هذا البحث لدراسة تأثير شكل الكانات (مربعة منفصلة – حلزونية مستديرة – حلزونية مربعة) وكذلك استخدام السلك الشبك الحديد على تحزيم العمود المربع القصير ذو قطاع مركب حديد. اشتمل البحث على دراسة عملية ونظرية باستخدام برنامج تحليل عددي (ANSYS 15). الأعمدة المستخدمة في الدراسة ذات قطاع مربع 15 سم * 15 سم و بارتفاع 90 سم و تسليح داخلي 4 أسياخ رأسية بقطر 8 مم و كانات بقطر 6 مم و كمره حديد بقطاع IPE NO. 80. تبين من نتائج الاختبارات العملية أن الكانات الحلزونية المربعة أعطى أفضل نتيجة حيث زادت قدرة التحمل القصوى للعمود بنسبة تراوحت من 9.10 % إلى 16.38 % مقارنة بالحمل الأقصى للعمود CS₁، بينما في حالة استخدام كانات حلزونية مستديرة بدون سلك شبك أدى إلى نقص قدرة التحمل القصوى للعمود بنسبة -3.75 %. أدى استخدام السلك الشبك إلى زيادة قدرة التحمل القصوى للعمود بنسبة 6.26 % ، 7.28 % ، 4.65 % في حالة الكانات المربعة المنفصلة و الكانات الحلزونية المربعة و الكانات الحلزونية المستديرة على الترتيب. أظهرت النتائج النظرية توافقاً مع النتائج العملية.

Abstract:

In recent years, the use of encased steel concrete composite columns has been increased significantly in medium and high-rise buildings. This paper investigates the axial compressive behavior of normal strength concrete of composite reinforced concrete steel columns confined by using different techniques. In this experimental program, six composite reinforced concrete steel columns of 150 mm×150 mm cross-section and 900 mm total height were casted. All composite columns have steel I section IPE No.80. Reinforced columns have four normal mild steel bars 8 mm diameter. Reinforced columns were provided with three different types of stirrups (square separate, square spiral and circular spiral) have 6 mm diameter @ 120 mm spacing. The deflection, strain, failure load and failure mode of the columns were discussed. The results showed that the new strengthening technique for composite column reinforced concrete steel column CS₆ with steel I section strengthened by spiral square stirrups and 2 layers of steel wire mesh has resulted an increase in the ultimate load carrying capacity about 16.33 % of the ultimate load carrying capacity of composite column CS₁. For strengthening technique for composite columns CS₂ strengthened by steel wire mesh stirrups has resulted an increase in the ultimate load about 6.26 % of the ultimate load of composite column CS₁ and

showed decreases in the deflection of control composite column. The spiral stirrups and steel wire mesh work to strap the composite columns, which increase the workability of concrete around the steel I section, that caused increase of the ultimate load.

Keywords: Composite, reinforced, column, steel, IPE, behavior, confinement, stirrups, spiral, experimental, FEA, Nonlinear, ANSYS

1. Introduction

Composite column is a structural member that uses a combination of structural steel shapes, pipes or tubes with or without reinforcing steel bars and concrete to provide adequate load carrying capacity to sustain either axial compressive loads alone or a combination of axial loads and bending moments. The steel-concrete composite column has been widely used in structural engineering practice for its great load bearing capacity and ductility. In a composite column both the steel and the concrete sections resist the external loading by interacting together by bond and friction. Composite columns are constructed providing structural steel inside concrete or concrete inside the structural steel. These columns are being used worldwide for the construction of medium and high-rise buildings since it can reduce the size of the columns in the building and increase the usable space of the floor plan. **Tokgoz et al. (2008)** conducted experimental research on the eccentric compression performance and the axial compression performance of long SRCC. A theoretical analysis method that took material nonlinearity into account was proposed and verified by test results. The calculated results agreed well with the experimental results. **Kim et al. (2012)** tested Seven concrete-encased steel columns using high-strength steel (nominal yield strength $f_y = 913$ and 806 MPa) and high-strength concrete (cylinder compressive strength $f_c' = 94$ and 113 MPa) to investigate the eccentric axial load-carrying capacity and the deformation capacity. The test parameters were full or partial concrete-encasement, the eccentricity of the axial load, and the effect of lateral reinforcement. Because the yield strain (approximate to 0.004) of the high-strength steel is greater than the ultimate compressive strain (approximate to 0.003) of the concrete subjected to short-term loads, the current study focused on the effect of early concrete crushing on the behavior of the composite columns. The test results showed that in the case of inadequate lateral confinement, the load-carrying capacity was limited by the early crushing of concrete. However, because of the high-strength steel section, all test specimens showed ductile flexural behavior after the delamination of the concrete. The test results were compared with the predictions by nonlinear numerical analysis and current design codes. **Zhu et al. (2014)** carried out an experimental study on the axial compression performance of steel reinforced concrete columns (SRCC). Test results showed that stirrups had no effects on the ultimate compressive strength of SRCC; however, they could greatly enhance the ductility and residual strength of the SRCC. **El-Kholy Ahmed M. et al. (2015)** presented a practical confinement configuration consisting of single Expanded Metal Mesh (EMM) layer in addition to regular tie reinforcement. The EMM layer was warped above ties. The specimens

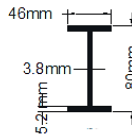
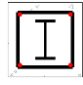

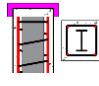
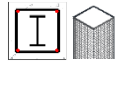
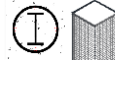
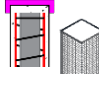
were cast in vertical position simulating the construction field and they were tested under concentric compression till failure. The results indicated that the columns, confined with proposed lateral reinforcement, revealed significant improvement in the strength and ductility. Also, high reduction in ties volumetric ratio with no loss in ultimate load could be achieved by installing the EMM layer. **Campian et al. (2015)** reported a series of experimental studies on SRCCs made of high-strength steel reinforcement and high-strength concrete. Research results showed that the material strength of steel in the composite column was not fully developed because the ultimate compressive strain of concrete was only 0.0033. **Juraj Frólo et al. (2016)** presented some results of theoretical and experimental investigations of composite steel-concrete columns with solid steel profiles - steel cores. Due to absence of simplified design method according to EN 1994-1-1, design of these columns in practice is limited in general. Reasons for this are residual stresses in steel profile caused by fabrication process and limitation of strains in concrete. Recommendations have been determined for simplified design method according to EN 1994-1-1 for composite columns made of high strength concrete filled steel tube with central steel core. Results of experimental research on composite columns with the cross-section made of steel core covered by reinforced concrete are presented. **Rahman Md. Soebur et al. (2016)** presented an experimental and numerical investigations of the behavior of concrete encased steel composite columns subjected to short-term axial load. Eleven short fully encased composite columns with square shaped cross section were constructed and tested to examine the load deflection behavior. The main variables in the test were considered as concrete compressive strength, cross sectional size and percentage of structural steel. A nonlinear 3-D finite element (FE) model has been developed to analyses the inelastic behavior of steel, concrete, and longitudinal reinforcement as well as the effect of concrete confinement of the fully encased composite columns. FE models have been validated against the current experimental study conduct in the laboratory and published experimental results under concentric load. It has been observed that FE model is able to predict the experimental behavior of fully encased composite columns under concentric gravity loads with good accuracy. Good agreement had been achieved between the complete experimental and the numerical load-deflection behavior in this study. The capacities of each constituent of FEC columns such as structural steel, concrete and rebar's were also determined from the numerical study. Concrete was observed to provide around 57% of the total axial capacity of the column whereas the steel I-sections contributes to the rest of the capacity as well as ductility of the overall system. The nonlinear FE model developed was also used to explore the effect of concrete strength and percentage of structural steel on the behaviour of FEC columns under concentric loads. The axial capacity of FEC columns had been found to increase significantly by increasing the strength of concrete. **Lele Sun et al. (2020)** presented test results on Steel Reinforced Concrete Column with Welded Stirrups (SRCC-WS). The SRCC-WS had no longitudinal steel bars to reduce the labor forces and avoid the difficulty in connecting longitudinal bars at construction site, and stirrups were welded directly to the steel reinforcement to ensure they worked together. Five SRCC-WSs were tested under axial

compression; and two traditional Steel Reinforced Concrete Columns (SRCCs) were tested for comparison. Failure modes, load displacement curves, and strain evolution curves measured from tests were presented. Test results showed that the ultimate axial compression strength and ductility of a SRCC-WS was a little higher than that of a SRCC having the same overall steel ratio. A simplified design method for calculating the effective lateral confined pressure on the core concrete provided by the combined action of welded stirrups and steel reinforcement flanges was proposed. The calculated yield compression strength of a SRCC-WS based on the proposed concrete model agreed better with the experimental value than that calculated by the method in Eurocode 4. **Jianyang Xue et al. (2020)** presented the seismic performance of High-strength Concrete Encased Steel columns with Rectangular - spiral Stirrups (HCESRS). The composite specimen was tested under reverse cyclic loading and numerically simulated by the finite element method. Using ABAQUS software, numerical analysis of the specimen was performed, including hysteresis curve, skeleton curve, stress comparison and energy dissipation. Experimental results were compared with the numerical simulation to verify the accuracy of the numerical analysis. The influence of parameter changes such as shear span ratio, axial compression, steel content of I-shape and steel yield strength of HCESRS column were investigated. It was found that as the shear span ratio increases, the ultimate bearing capacity of the member decreases and the deformation capacity increases. Due to the brittle failure characteristics of high strength concrete, the limit value of axial compression ratio of HCESRS column was systematically studied, and effect of axial compression ratio on the ductility for HCESRS column has been investigated. This numerical analysis reliably evaluated and analyzed the seismic response of the HCESRS column. **Gosala Sai Ram Reddy et al. (2021)** presented an experimental and numerical studies on the structural behavior of Concrete Filled Steel Tube (CFST) and Reinforced Cement Concrete (RCC) stub columns of different concrete grade. The experimental result of rectangular and square stub column of both RCC and CFST have been compared with a Finite Element (FE) study using ABAQUS platform. The comparison results show that the axial capacity of the CFST stub columns on an average is 50% and 55% more than the RCC stub columns with square section and circular sections respectively. Also, the effect of thickness of steel tubes, concrete cube strength and steel percentage is also studied.

2. Experimental program

In this experimental program, six composite reinforced concrete steel columns of 150 mm×150 mm cross-section and 900 mm total height were casted. Reinforced columns have four normal mild steel bars 8 mm diameter. Reinforced columns were provided with three different types of stirrups (square separate, square spiral and circular spiral) have 6 mm diameter @ 120 mm spacing. The loads were applied concentrically on top of the columns. The tested columns are shown in Table [1]

[Table 1] List of new strengthening techniques of composite columns

Col. Code	Col. Dim.	Vertical Reinforcement	Key	Stirrups Φ 6 mm / 12cm	Steel Wire mesh
CS_1	150 X 150 X 900 mm	4 Φ 8 mm + Steel I Section  46 x 80 mm ----- 5.2 x 3.8 mm		Square Separate	----
CS_2				Circular Spiral	----
CS_3				Square Spiral	----
CS_4				Square Separate	2 Layers
CS_5				Circular Spiral	2 Layers
CS_6				Square Spiral	2 Layers

(CS_1) composite reinforced concrete-steel column with steel IPE No. 80 section [46x80x5.2x3.8 mm] as shown in figure 1 and 2. The behavior of this column used as a basis for comparison to evaluate the performance benefits achieved using different technique as shown in [Figure 1 and 2].

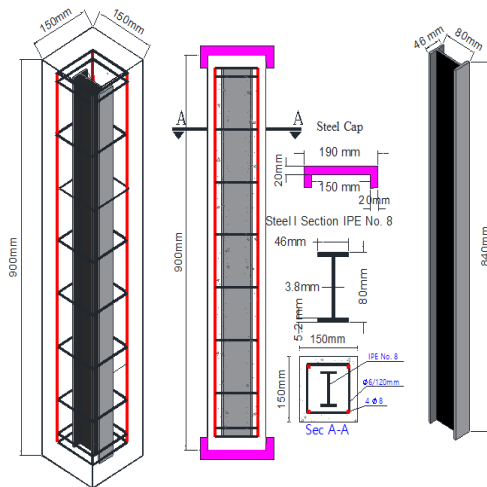


Figure 1. Detailing of composite column CS_1



Figure 2. Detailing of composite column CS_1

(CS_2) composite reinforced concrete-steel column with one steel IPE No. 80 section [46x80x5.2x3.8 mm] with circular spiral stirrups Φ 6 @ 80 mm as shown in [Figure 3].

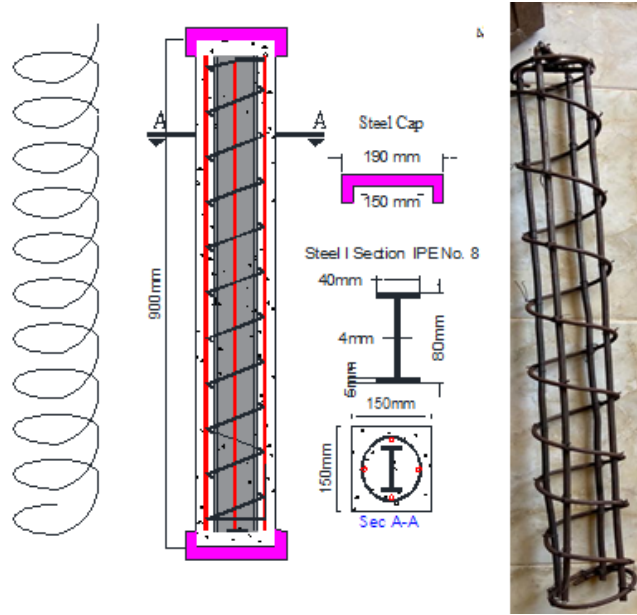


Figure 3. Detailing of control composite column CS_2

(CS_3) reinforced concrete-steel composite column with steel IPE No. 80 section [46x80x5.2x3.8 mm] confined with square spiral stirrups as shown in [Figure 4 and 5].

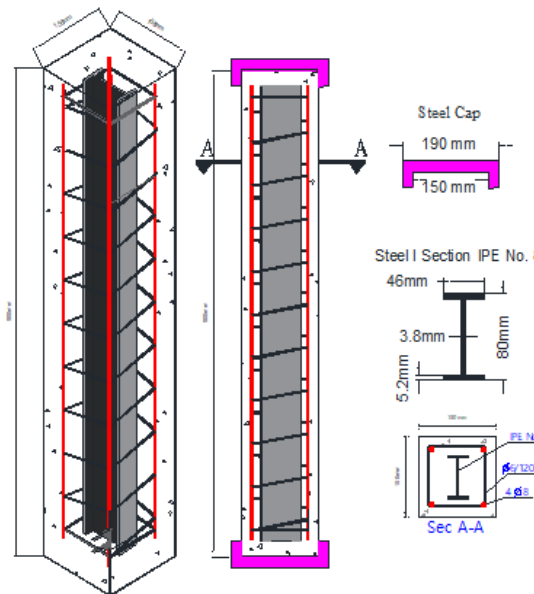


Figure 4. Detailing of composite column CS_3



Figure 5. Detailing of composite column CS_3 .

(CS_4) composite reinforced concrete-steel column with steel IPE No. 80 section [46x80x5.2x3.8 mm] with square separate stirrups confined by 2 layers of steel wire mesh as shown in [Figure 6 and 7].

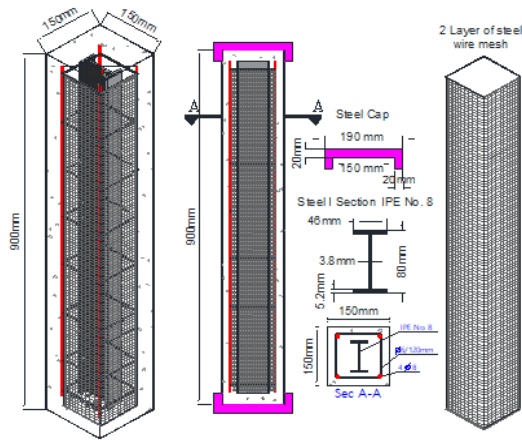


Figure 6. Detailing of composite column **CS₄**.



Figure 7. Detailing of composite column **CS₄**

(**CS₅**) composite reinforced concrete-steel column with steel IPE No. 80 section [46x80x5.2x3.8 mm] confined with circular spiral stirrups Φ 6 @ 80 mm and 2 layers of steel wire mesh as shown in [Figure 8].

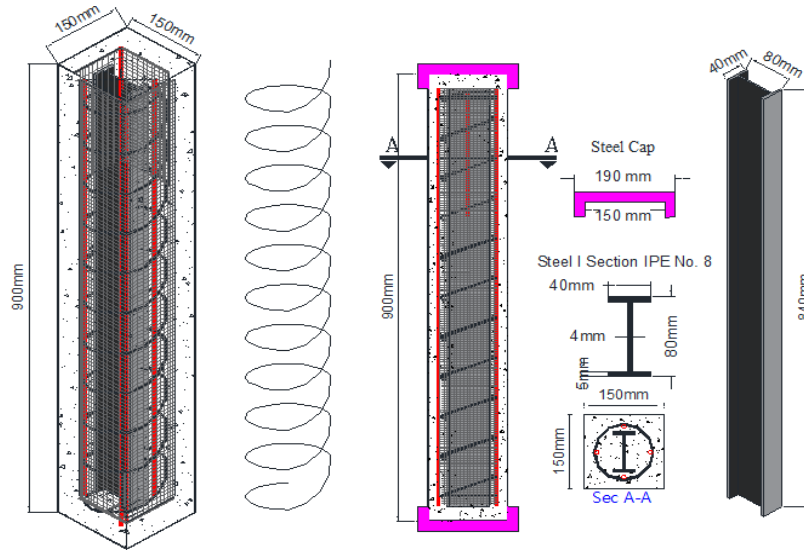


Figure 8. Detailing of composite column **CS₅**.

(**CS₆**) composite reinforced concrete-steel column with steel IPE No. 80 section [46x80x5.2x3.8 mm] confined with square spiral stirrups and 2 layers of steel wire mesh. as shown in [Figure 9].

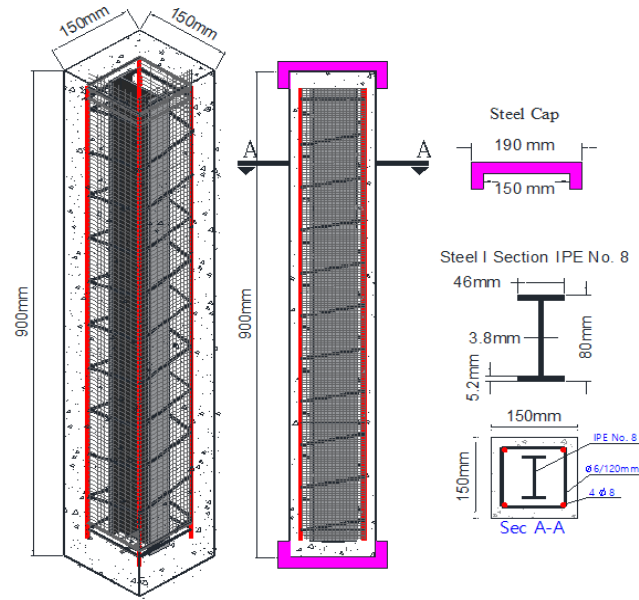


Figure 9. Detailing of composite column **CS₆**.

A. Concrete mixing design, casting and curing

The concrete mix was designed to obtain target strength of 30 N/mm^2 at the age of 28 days. The concrete mix used in all specimens was designed according to the Egyptian code of practice. The average time of mixing concrete in the mixer was from 4 to 6 min from the moment of adding water. Before each casting the wood forms were prepared and lubricated with oil. During casting, a mechanical vibrator was used to compact the concrete. All column specimens were left in forms for 24 hours then all of sides were removed and covered with wet canvas for 28 days to achieve the expected strength. Six standard cubes $150 \times 150 \times 150 \text{ mm}$ were casted from each concrete patch to define the concrete properties. The curing conditions for the cubes were the same the column specimens' condition

B. Test setup and loading

Before starting casting and while preparing the reinforcement of composite columns, the strain gauges were fixed directly on the vertical reinforcement, on the steel stirrups and on the steel I section. Before testing, the composite columns were washed by a thin coat of white plaster to determination and mapping the cracks at the different stages of loading. One LVDT of accuracy 0.01 mm (deflection) were used, was fixed directly under the cap to determine the deflection as shown in Figure 6. After the columns were accurately facilitate placed into position on the testing machine, the initial readings from the LVDT were taken before the load application.



Figure 10 Test loading.

C. Test procedure

The zero load readings for the vertical steel bars strain, stirrups steel strain and steel I section strain were recorded. The load was applied in regular increments from zero up to the failure load. At the end of each load increment, readings from the load cell and strain gauges were recorded through the data acquisition system. The tests were terminated by complete destruction of the column specimen.

D. Measurements

The followings were measured:

- i. The load readings were taken for all stages.
- ii. The LVDT readings were taken for all load stages
- iii. The strain gauge readings were taken for all load stages.
- iv. Crack patterns at different load levels were monitored until columns failure.

3. Finite element modeling

The present study addresses a three-dimensional nonlinear finite element analysis (FEA) modeling for the prediction of the shear behavior of composite reinforced concrete steel column confined with various stirrups shape and steel wire mesh. The nonlinear FEA was performed using the ANSYS program. Eight nodes 3-D space solid elements were used to represent the concrete. The steel reinforcements were modeled as discrete reinforcing steel bars using two nodes 3-D space link element.

A. Reinforcement concrete

Concrete and resin were modeled using 3-D (8-node) solid elements. This element is capable of considering cracking in three perpendicular directions, plastic deformation and crushing, and creep. The element is defined by eight nodes having three translation degrees of freedom at each node in the x, y and z directions.

B. Steel reinforcement

A Link180 element was used to model the steel reinforcement. Two nodes are required for this element. Each node has three degrees of freedom translations in the nodal x, y, and z directions. The element is also capable of plastic deformation.

C. Steel I Section

An eight-node solid element, Solid185, was used for the steel plates at the supports in the beam models. The element is defined with eight nodes having three degrees of freedom at each node translations in the nodal x, y, and z directions. The geometry and node locations for this element type.

D. Concrete

Concrete is considered as a quasi-brittle material. Complete stress-strain curves of concrete are needed to accurately predict structural behavior to failure and post-failure. ECP 203-2007 constructs the simplified uniaxial compressive stress-strain curve, as shown in Fig. 11, for concrete used in this finite element model. Poisson's ratio for concrete was assumed to be 0.2 for all four beams as denoted in ECP 203 2007. Typical shear transfer coefficients range from (0.0 to 1.0), with 0.0 representing a smooth crack (complete loss of shear transfer) and 1.0 representing a rough crack (no loss of shear transfer). When the element is cracked or crushed, a small amount of stiffness is added to the element for numerical stability.

E. Steel reinforcement

The reinforcement element was assumed to be a bilinear isotropic elastic-perfectly plastic material and identical in tension and compression as shown in Fig. 12. Modulus of elasticity and Poisson's ratio were taken 2×10^5 MPa and 0.3 respectively, for all types of steel reinforcement.

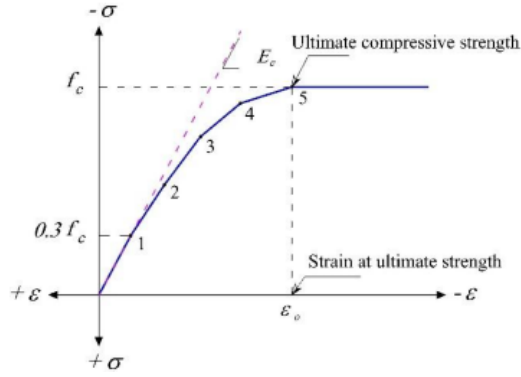


Figure 11 Simplified compressive uniaxial stress-strain curve for concrete

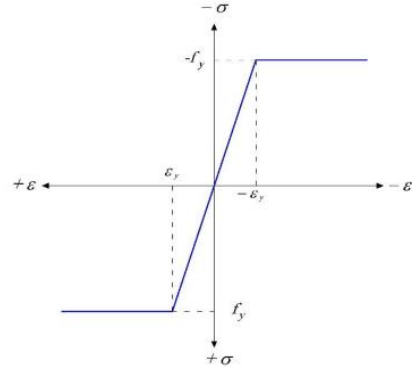


Figure 12 Stress-strain relationship of steel rebar

F. Finite Element Model

The finite element model is used to represent six specimens with cross section 150 x 150 mm and 900 mm height were represented. Figures 13, 14, 15, 16, 17 and 18 show the modeling and detailing of composite reinforced concrete-steel column CS₁, CS₂, CS₃, CS₄, CS₅ and CS₆ respectively.

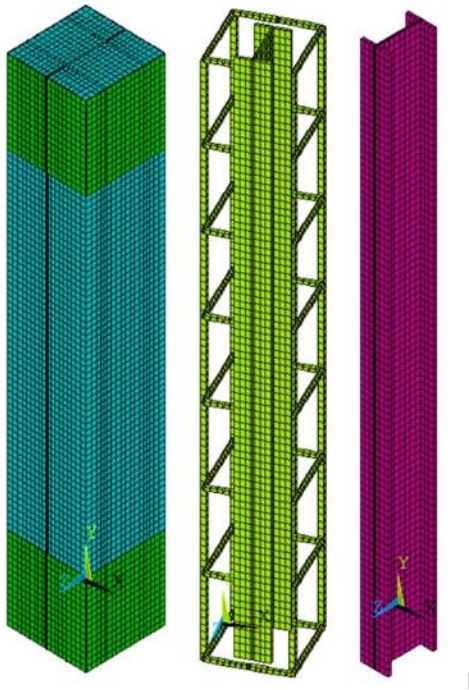


Figure 13 modeling and detailing of column [CS₁]

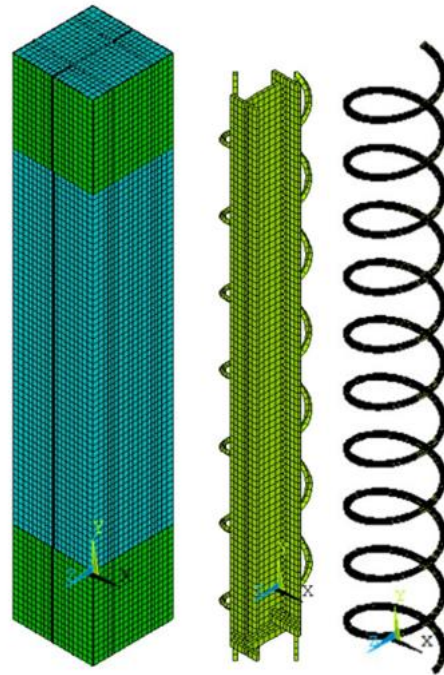


Figure 14 modeling and detailing of column [CS₂]

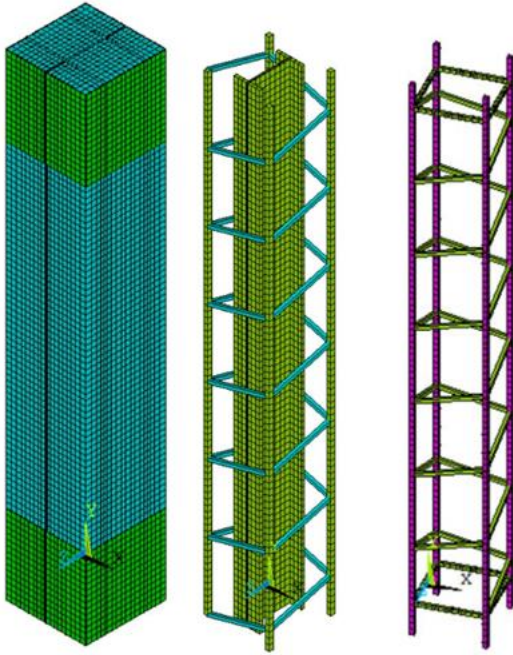


Figure 15 modeling and detailing of column [CS₃]

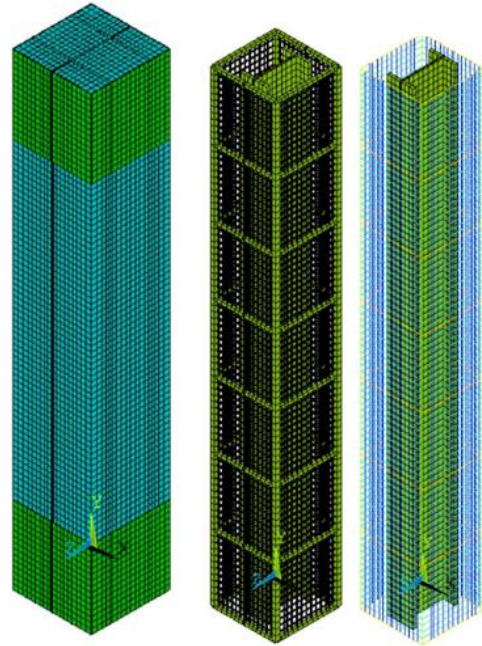


Figure 16 modeling and detailing of column [CS₄]

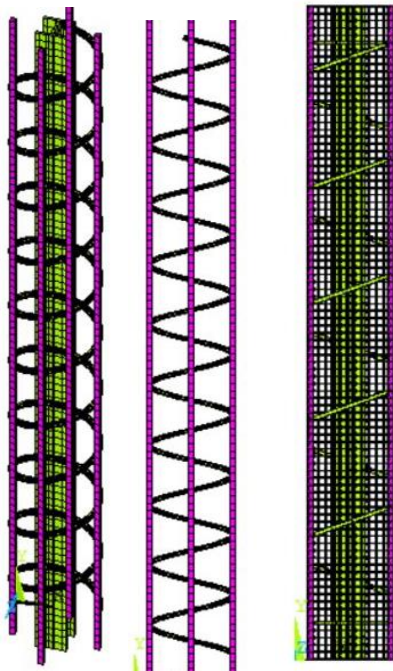


Figure 17 modeling and detailing of column [CS₅]

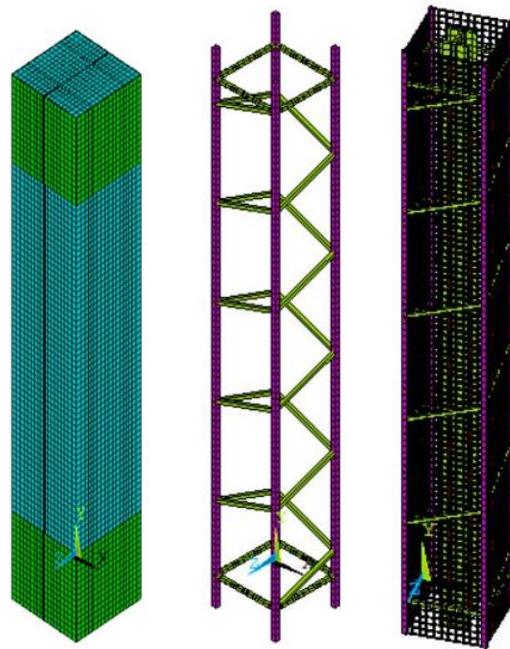
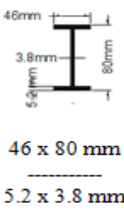








Figure 18 modeling and detailing of column [CS₆]

4. Results and analysis of experimental and finite element model results

The comparison of ultimate load carrying capacity (failure load) obtained from experimental (EXP) and finite element (FEA) analysis as shown in Table (3).

Table (3) shows the comparison of the maximum failure load obtained from experimental (EXP) and finite element (FEA) analysis.

Col. Code	Col. Dim.	Vertical Reinforcement	Key	Stirrups Φ 6 mm / 12cm	Steel Wire mesh	Ultimate load carrying capacity of column [kN]		% Increase or decrease in load carrying capacity of CS ₁	
						Exp.	FEA	Exp.	FEA
CS ₁	150 X 150 X 900 mm	4 Φ 8 mm + Steel I Section 		Square Separate	---	910.52	900	0.00	0.00
CS ₂				Circular Spiral	---	876.30	865.00	-3.75	-3.88
CS ₃				Square Spiral	---	993.40	972.00	+9.10	+8.00
CS ₄				Square Separate	2 Layers	967.52	930.00	+6.26	+300
CS ₅				Circular Spiral	2 Layers	919.60	915.00	+0.90	+1.60
CS ₆				Square Spiral	2 Layers	1059.70	1023.00	+16.38	+13.66

Comparison of the results is displayed in the following Tables and Figures:

- Figure 19 shows a comparison of load capacity for CS₁, CS₂, CS₃, CS₄, CS₅ and CS₆.
- Figure 20 shows the relationship between load and strain gauge at stirrups and vertical reinforcement for composite column (CS₁), (CS₂), (CS₃), (CS₄), (CS₅) and (CS₆).
- Fig. 21 shows the relationship between load and strain gauge at flange of steel I Section for composite column (CS₁), (CS₂), (CS₃), (CS₄), (CS₅) and (CS₆).

The results showed that the composite column (CS₃) with steel I section strengthened by square spiral stirrups has resulted an increase in ultimate load by 9% of the ultimate load carrying capacity (failure load) of column (CS₁) and the composite column (CS₆) with steel I section strengthened by square spiral stirrups and 2 layers of steel wire mesh has resulted an increase in ultimate load by 16.38 % of the ultimate load carrying capacity of column (CS₁). The composite column (CS₄) confined with 2 layers of steel wire mesh has resulted an increase in ultimate load carrying capacity by 6.26 % of the ultimate load carrying capacity of column (CS₁). The composite column (CS₅) with steel I section strengthened by circular spiral stirrups and 2 layers of steel wire mesh has resulted an increase in ultimate load carrying capacity by 1 % of the ultimate load of column (CS₁).

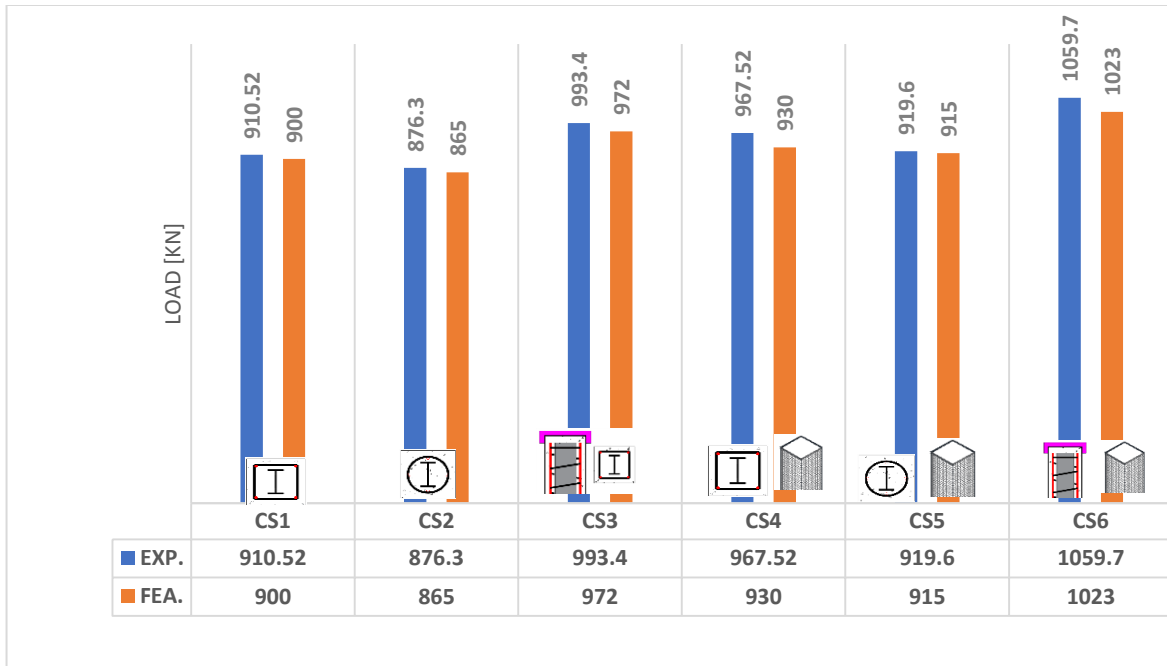


Figure 19 Comparison of load capacity for CS₁, CS₂, CS₃, CS₄, CS₅ and CS₆.

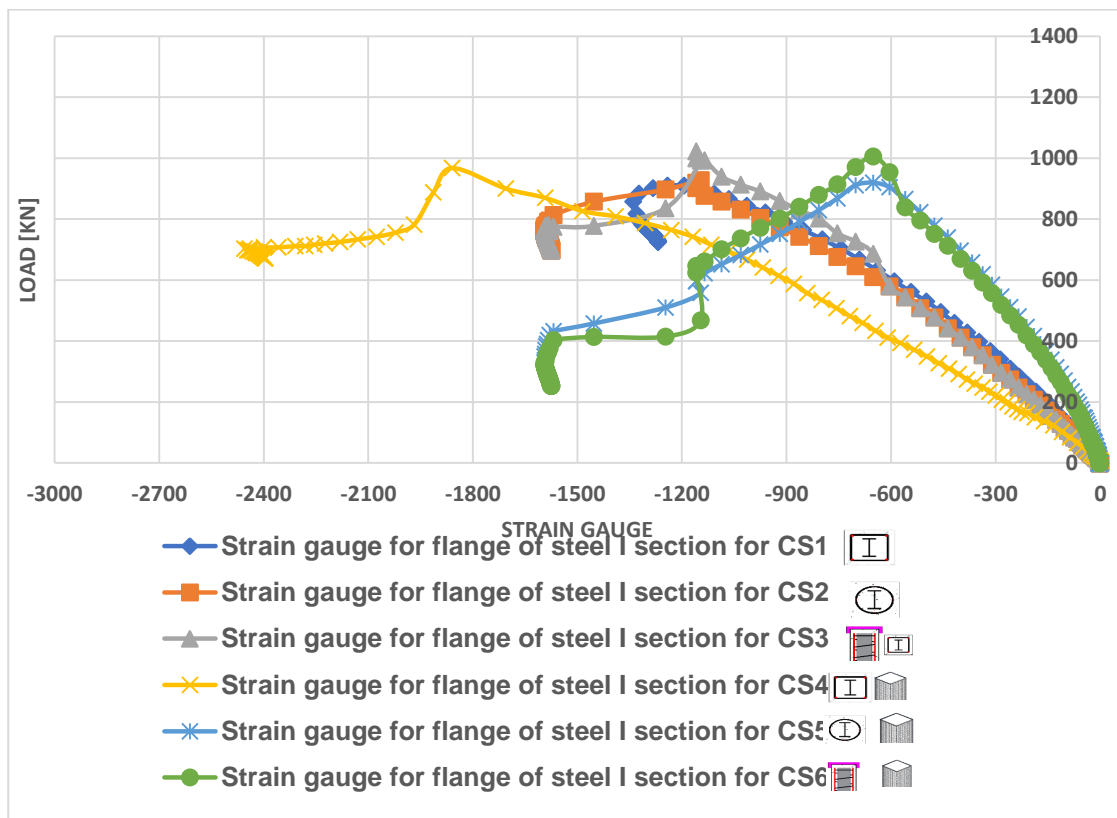


Figure 20 the load-strain relationship (at internal stirrups and vertical reinforcement) for composite columns (CS₁), (CS₂), (CS₃), (CS₄), (CS₅) and (CS₆).

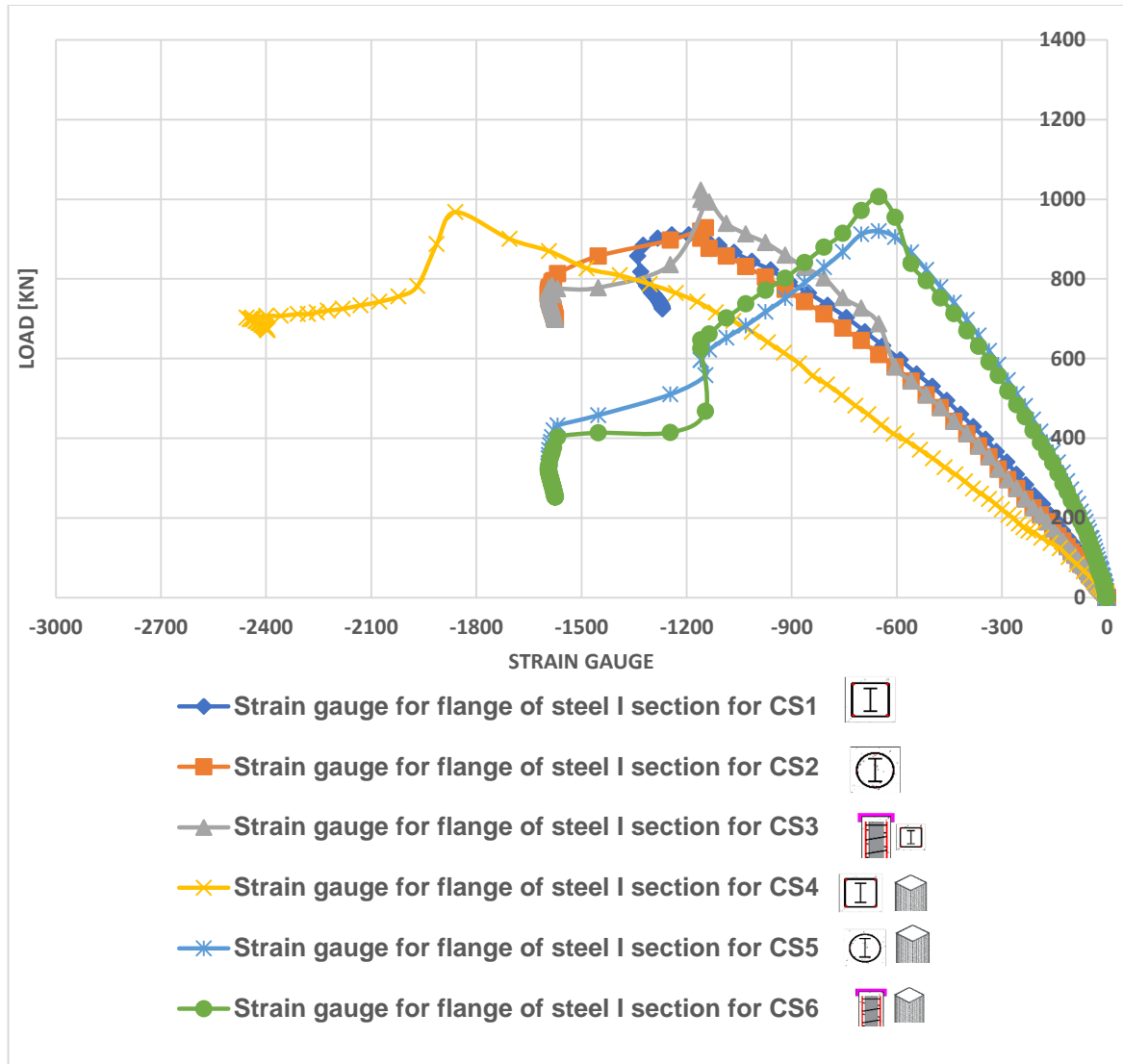


Figure 21 the relationship between load and strain gauge at flange of steel I Section for composite columns (CS₁), (CS₂), (CS₃), (CS₄), (CS₅) and (CS₆).

- Fig 22 shows the comparison between the experimental results and FEA results of the load-Strain relationship at Vertical reinforcement for the composite columns (CS₁) and (CS₄).
- Fig 23 shows the comparison between the experimental results and FEA results of the load-Strain relationship at Vertical reinforcement for the composite columns (CS₂) and (CS₅).
- Fig 24 shows the comparison between the experimental results and FEA results of the load-Strain relationship at Vertical reinforcement for the composite columns (CS₃) and (CS₆).

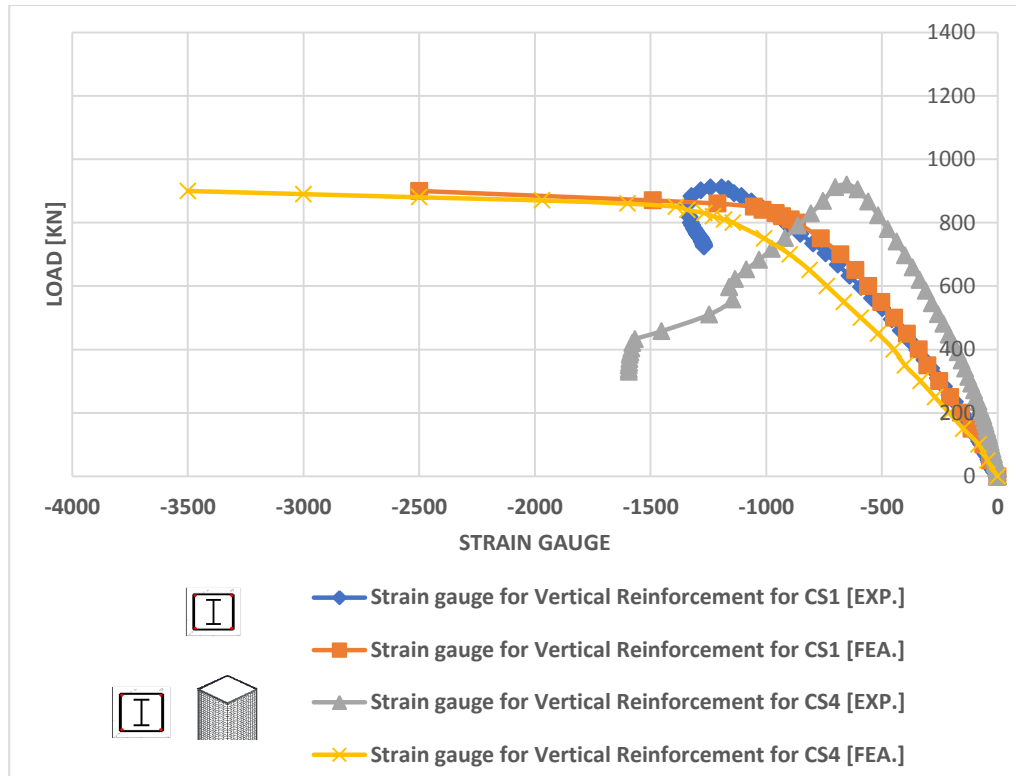


Figure 22 comparison between the experimental results and FEA results of the load-Strain relationship at Vertical reinforcement for the composite columns (CS₁) and (CS₄).

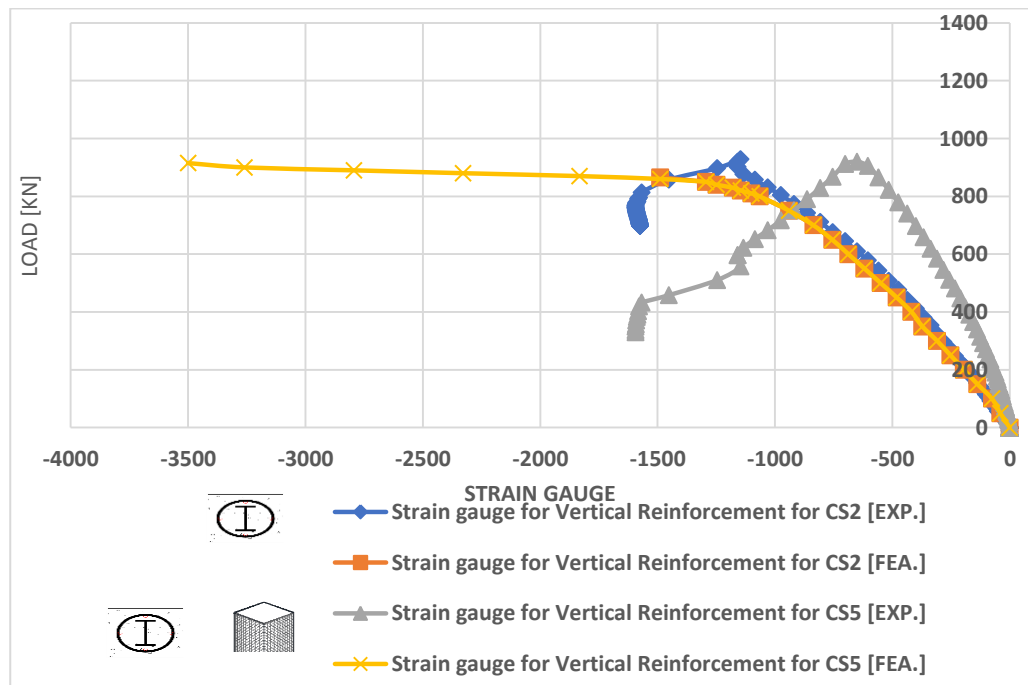


Figure 23 comparison between the experimental results and FEA results of the load-Strain relationship at Vertical reinforcement for the composite columns (CS₂) and (CS₅)

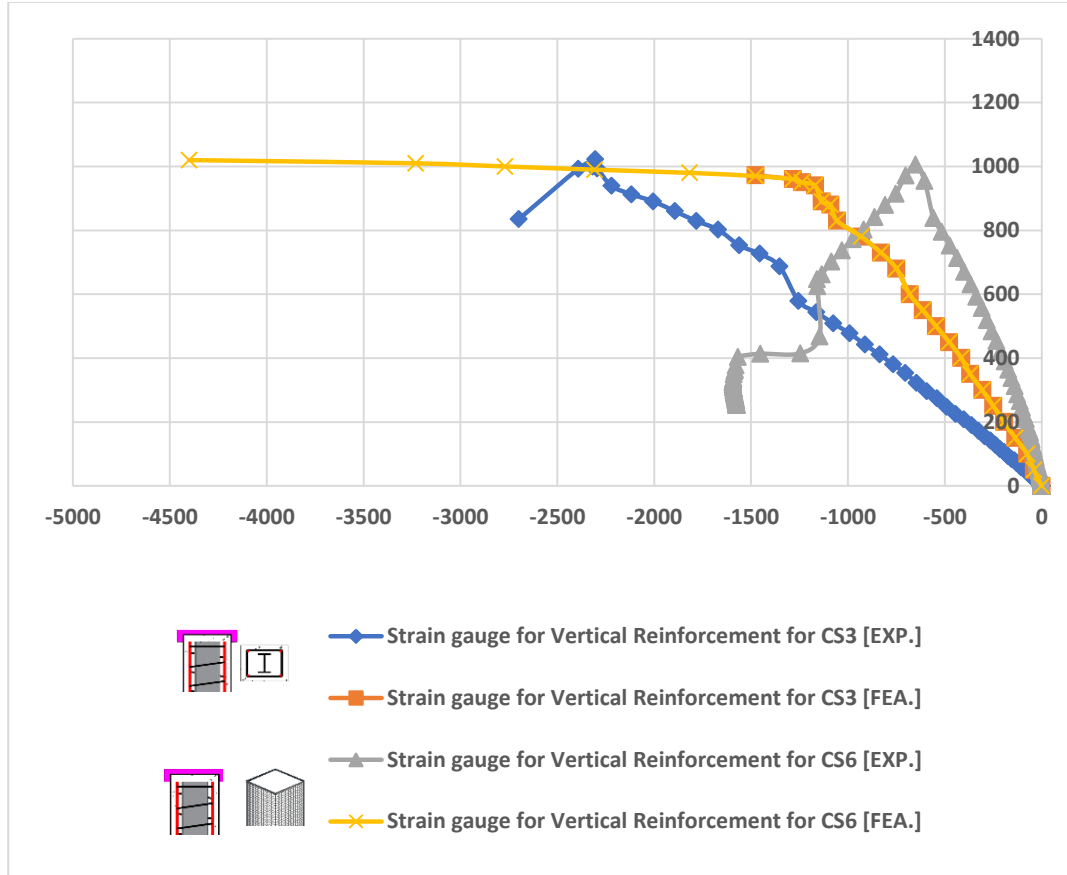


Figure 24 comparison between the experimental results and FEA results of the load-Strain relationship at Vertical reinforcement for the composite columns (CS₃) and (CS₆).

5. Failure modes

Control composite column CS₁

The composite column (CS₁) with steel I section tested axial load is used as a basis for comparison to evaluate the performance benefits achieved using confinement technique.

For the specimen (CS₁), the failure occurred in concrete due to shear failure in the top third of the column height as shown in Figure 25 and 26.

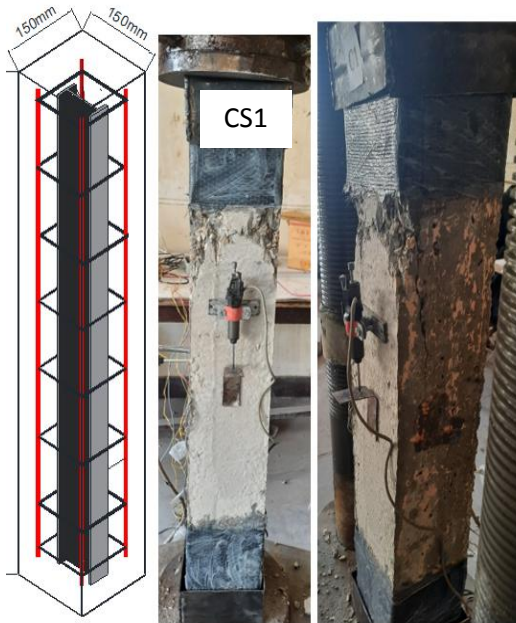


Figure 25 Crack pattern of control composite column (CS₁) EXP.

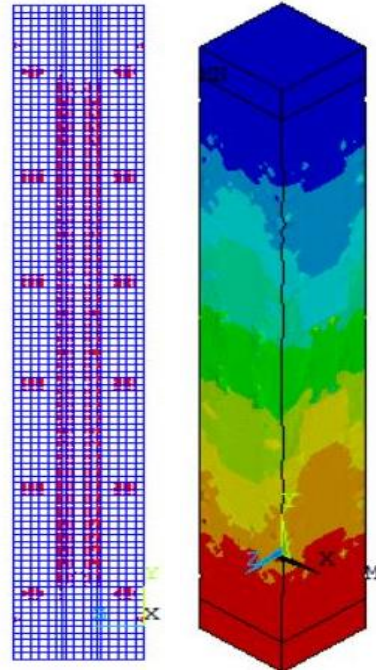


Figure 26 Crack pattern of control composite column (CS₁) FEA.

Composite column (CS₂)

The composite column (CS₂) confined with circular spiral stirrups was tested under axial load. The failure of composite column (CS₂) occurred in concrete due to shear failure in the top and bottom third of the column height as shown in Fig. 27 and 28

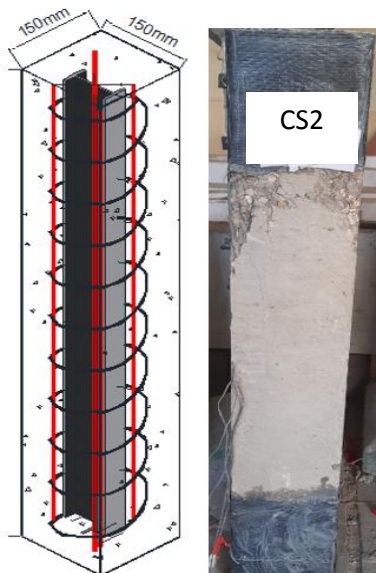


Figure 27 Crack pattern of control composite column (CS₂) EXP.

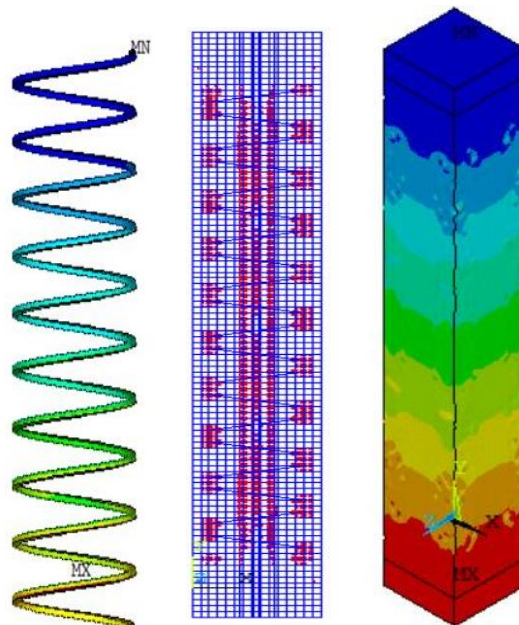


Figure 28 Crack pattern of control composite column (CS₂) FEA.

Composite column (CS₃)

The composite column (CS₃) confined with square spiral stirrups was tested under axial load. The failure of composite column (CS₃) occurred in concrete due to shear failure in the top and bottom third of the column height as shown in Fig. 29 and 30.

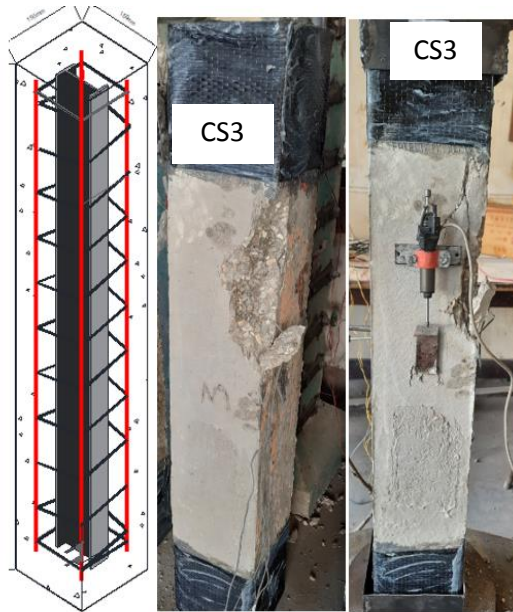


Figure 29 Crack pattern of composite column (CS₃) confined with square spiral stirrups EXP.

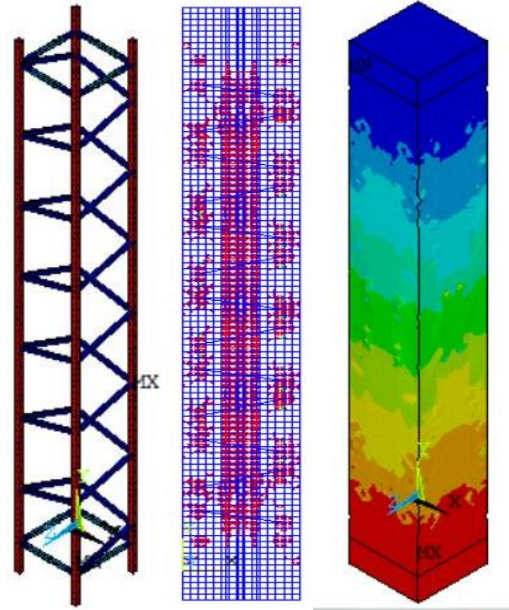


Figure 30 Crack pattern of composite column (CS₃) confined with square spiral stirrups FEA.

Composite column (CS₄)

The composite column (CS₄) confined with two layers of steel wire mesh was tested under axial load. The failure of composite column (CS₄) occurred due to shear failure in the middle of the column Height as shown in Fig. 31, 32 and 33. These figures show that the cracks started at the middle of the column for both experimental and finite element model.



Figure 31 crack pattern of composite column (CS₄) confined with 2 layer of steel wire mesh.

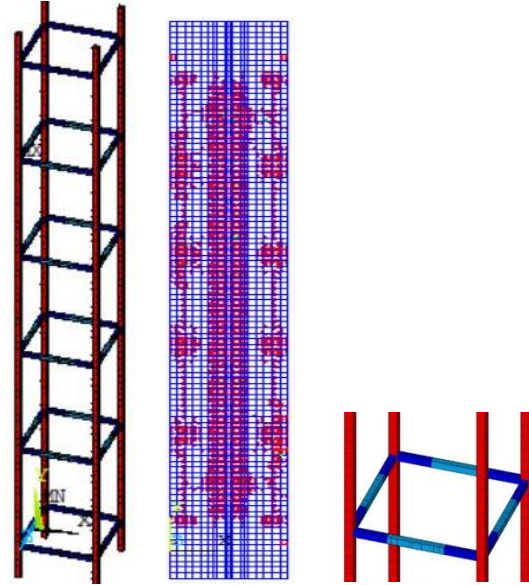


Figure 32 crack pattern of composite column (CS₄) confined with 2 layer of steel wire mesh FEA.

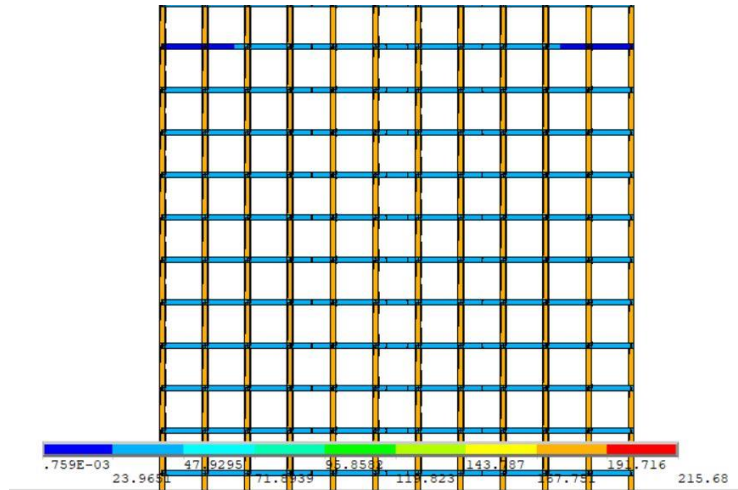


Figure 33 stresses of composite column (CS₄) confined with 2 layer of steel wire mesh FEA.

Composite column (CS₅)

The composite column (CS₅) confined with circular spiral stirrups and 2 layers of steel wire mesh was tested under axial load. The failure of composite column (CS₅) occurred in concrete due to shear failure in the top and bottom third of the column height as shown in Fig. 34.

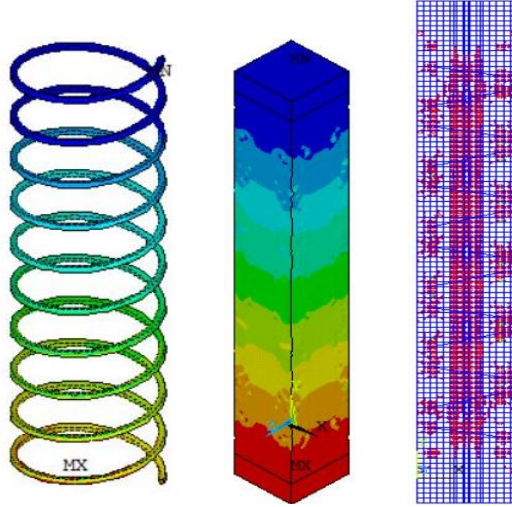


Figure 34 crack pattern of composite column (CS₅) confined with 2 layer of steel wire mesh FEA.

Composite column (CS₆)

The composite column (CS₆) confined with square spiral stirrups and 2 layers of steel wire mesh was tested under axial load. The failure of composite column (CS₆) occurred in concrete due to shear failure in the top and bottom third of the column height as shown in Fig. 35 and 36.

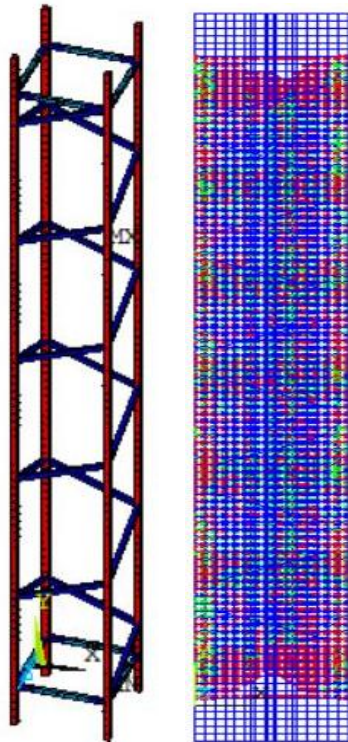


Figure 35 crack pattern of composite column (CS₆) confined with square spiral stirrups and 2 layers of steel wire mesh was tested under axial load.

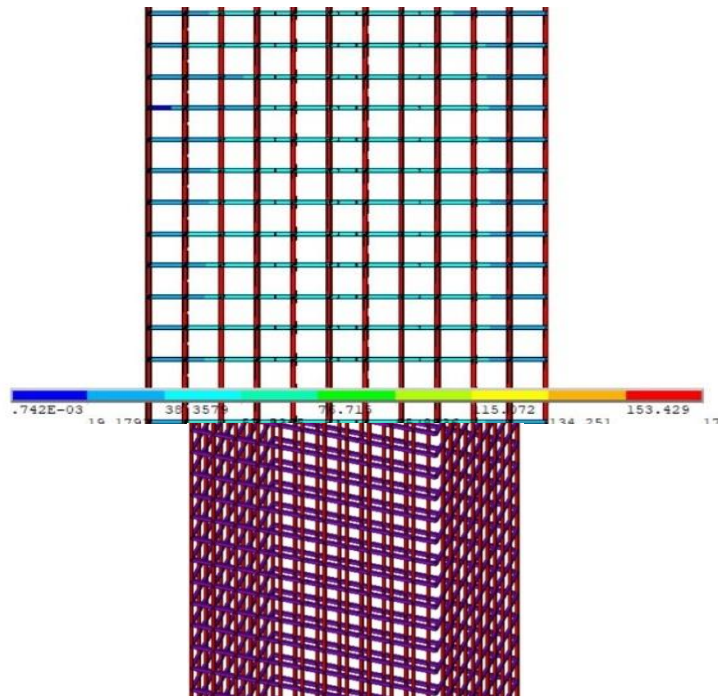


Figure 36 stresses of composite column (CS₆) confined with square spiral stirrups and 2 layers of steel wire mesh was tested under axial load.

6. Conclusions

From the present study, the followings have been concluded:

- The more effective and best technique is that composite column confined by using square spiral steel stirrups and 2 layers of steel wire mesh. An increase was obtained in the load capacity by 16.33 % of the composite column CS1 ultimate capacity and has an acceptable value of stiffness.
- For composite column confined with steel wire mesh (2 layers) an increase was obtained in the load capacity by 6.26 % of the composite column CS₁ ultimate capacity.
- The spiral stirrups and steel wire mesh work to strap the composite columns, which increase the workability of concrete around the steel I section, that caused increase of the ultimate load.
- Generally, a fair agreement has been obtained between experimental results and finite element analysis.

7. REFERENCES

1. Campian C, Nagy Z, Pop M. (2015), "Behavior of fully encased steel-concrete composite columns subjected to monotonic and cyclic loading", *Procedia Eng*;117 (3) : 439 – 51
2. El-Kholy Ahmed M.and Dahish Hany, A. B. (2016), "Improved confinement of reinforced concrete columns", Faculty of Engineering, Ain Shams University. Production and hosting by Elsevier B.V.
3. Gosala Sai Ram Reddy, Madhusudhan Bolla, M. Longshithung Patton and Dibyendu Adak (2021), "Comparative study on structural behaviour of circular and square section-Concrete Filled Steel Tube (CFST) and Reinforced Cement Concrete", *Structures* 29 (2021) 2067–2081
4. Jianyang Xue, Xiangbi Zhao, Xiaojun Ke, Xin Zhang, Fengliang Zhang and Peng Zhang (2020), "Experimental and numerical investigation of high-strength concrete encased steel columns with rectangular-spiral stirrups", *Journal of Building Engineering* 32, 101518.
5. Juraj Frólo and Štefan Gramblička (2016), "Steel core in composite steel-concrete columns" *Key Engineering Materials* Submitted: 2015-10-12 ISSN: 1662-9795, Vol. 691, pp 195-DOI= <http://doi.acm.org/10.1145/332040.332491>.
6. Kim CS, Park HG, Chung KS, Choi IR. (2012) "Eccentric axial load testing for concreteencased steel columns using 800 MPa steel and 100 MPa concrete.", *J Struct” Eng, ASCE*;138 (8) : 1019 – 31.
7. Lele Suna, Qijie Maa, Fei Hana, Zexin Liua, Jinglong Lia, Peijun Wanga, Hui Zhaob and Jian Sunb (2020), "Experimental investigation on axial compression behavior of steel reinforced", <https://doi.org/10.1016/j.engstruct.2019.109924>
8. Rahman Md Soebur and Mahbuba Begum (2016), "Numerical Simulations of Fully Encased Composite Columns under Gravity Loads", *Applied Mechanics and Materials*, Vol. 860, pp. 140-145, 2017 DOI: 10.4028/www.scientific.net/AMM.860.140
9. Tokgoz, S. and Dundar C. (2008), "Experimental tests on biaxially loaded concrete-encased composite columns.", *Steel Compos. Struct.* 2008; 8 (5) : 423 – 38.
10. Zhu WQ, Meng, G. and Jia JQ. (2014), "Experimental studies on axial load performance of highstrength concrete short columns.", *Proceedings of the Institution of Civil Engineers- Structures and Buildings* 2014; 167 (9) : 509 – 19.